Cell Stress and Chaperones (2023) 28:1001–1012
https://doi.org/10.1007/s12192-023-01394-1

ORIGINAL ARTICLE

Human HSP70-escort protein 1 (hHep1) interacts with negatively charged lipid bilayers and cell membranes

Milene N. O. Moritz[1] · Paulo R. Dores-Silva[1,2] · Amanda L. S. Coto[1] · Heloísa S. Selistre-de-Araújo[3] · Andrei Leitão[1] · David M. Cauvi[2] · Antonio De Maio[2] · Serena Carra[4] · Júlio Cesar Borges[1]

Received: 17 July 2023 / Revised: 9 November 2023 / Accepted: 10 November 2023 / Published online: 25 November 2023

Abstract

Human Hsp70-escort protein 1 (hHep1) is a cochaperone that assists in the function and stability of mitochondrial HSPA9. Similar to HSPA9, hHep1 is located outside the mitochondria and can interact with liposomes. In this study, we further investigated the structural and thermodynamic behavior of interactions between hHep1 and negatively charged liposomes, as well as interactions with cellular membranes. Our results showed that hHep1 interacts peripherally with liposomes formed by phosphatidylserine and cardiolipin and remains partially structured, exhibiting similar affinities for both. In addition, after being added to the cell membrane, recombinant hHep1 was incorporated by cells in a dose-dependent manner. Interestingly, the association of HSPA9 with hHep1 improved the incorporation of these proteins into the lipid bilayer. These results demonstrated that hHep1 can interact with lipids also present in the plasma membrane, indicating roles for this cochaperone outside of mitochondria.

Keywords HSP70s · Cochaperone · Heat Shock · Liposomes and plasma membrane

Introduction

70 kDa heat shock proteins (HSP70s) are molecular chaperones that participate in a large variety of cellular processes, including nascent protein folding, prevention of protein aggregation and transport of proteins through membranes (De Maio 1999; Hartl and Hayer-Hartl 2002). Studies have shown that HSP70s are associated with lipid membranes in several physiological and pathological events (Horváth et al. 2008; De Maio and Hightower 2021a), which has been proposed as an early event in their evolutionary pathway (De Maio and Hightower 2021b). Moreover, during cell stress, HSP70s can temporarily bind to membranes, re-establishing bilayer stability (Horváth et al. 2008) and activating the immune response (Vega et al. 2008). Intense investigation has been performed to elucidate the dynamics of the protein-lipid interaction of HSP70s with cellular phospholipid bilayers (Arispe et al. 2002, 2004; Broquet et al. 2003; Smulders et al. 2020). Ferrarini and collaborators detected the presence of HSP70s on the surface of several types of human tumour cells (Ferrarini et al. 1992; Multhoff et al. 1995). In addition, other studies have demonstrated HSP70s in cell membranes (Chouchane et al. 1994; Heufelder et al. 1992; Araujo et al. 2019; Salibe-Filho et al. 2020). Those findings pointed to the importance of the HSP70s imbalance in plasma membrane proteostasis, which may have deleterious consequences during the progression of diseases (Bailone et al. 2022; Samborski and Grzymisławski 2015; Turturici et al. 2011).

HSPA9 is the acronym for the human mitochondrial HSP70 that is also named mortalin or Grp75. HSPA9 has a differential subcellular distribution depending on the cell

Milene N. O. Moritz, Paulo R. Dores-Silva and Amanda L. S. Coto equally contributed for this work.

✉ Júlio Cesar Borges
borgesjc@iqsc.usp.br

1 São Carlos Institute of Chemistry, University of São Paulo – USP, P.O. Box 780, São Carlos, SP 13560-970, Brazil

2 Division of Trauma, Critical Care, Burns and Acute Care Surgery, Department of Surgery, School of Medicine, University of California San Diego, La Jolla, CA 92093, USA

3 Department of Physiological Sciences, Federal University of São Carlos, São Carlos, SP, Brazil

4 Centre for Neuroscience and Nanotechnology, Department of Biomedical, Metabolic and Neural Sciences, University of Modena and Reggio Emilia, Modena, Italy

conditions and can be located in mitochondria, endoplasmic reticulum, cytosol, cytoplasmic vesicles and plasma membranes (Ran et al. 2000; Wadhwa et al. 2002). In mitochondria, HSPA9 is involved in protein import, folding and degradation, and in extramitochondrial locations, it is involved in apoptotic pathways, cell metabolism and modulation of the immune system (Baseler et al. 2012; Kaul et al. 2007; Yun et al. 2017; Mazkereth et al. 2016).

The function of HSPA9, similar to other mitochondrial HSP70s, depends on a small cochaperone named HSP70-escort protein 1 (Hep1), which prevents the aggregation of HSPA9; without Hep1, mitochondrial biogenesis can fail (Burri et al. 2004; Sichting et al. 2005). In addition to preventing HSPA9 aggregation, human Hep1 (hHep1) is responsible for stimulating HSP70 ATPase activity and is an L-shaped protein with a zinc-finger-like motif (ZFLR). Through the heterologous coexpression of hHep1 and HSPA9, soluble recombinant HSPA9 can be produced in adequate amounts for performing experiments (Dores-Silva et al. 2015). Recently, our group demonstrated that in addition to being located in mitochondria, hHep1 is present in the nucleus (Dores-Silva et al. 2021b). Furthermore, hHep1 interacts with both negatively and positively charged liposomes and shows a noticeable preference for negatively charged liposomes prepared with lipids present in the inner mitochondrial membrane. (Dores-Silva et al. 2021b). This preference corresponds with previous findings showing that HSP70 exhibits a high selectivity for negatively charged phospholipids, particularly phosphatidylserine (Arispe et al. 2002, 2004; Armijo et al. 2014; Schilling et al. 2009). Specifically, HSPA9 interacts with negatively charged liposomes composed of phosphatidylserine and cardiolipin (Dores-Silva et al. 2020b). Together, these findings provide an opportunity to investigate whether and how hHep1 interacts with lipid bilayers, similar to HSPA9. In this context, the aim of the study was to further elucidate how hHep1 interacts with negatively charged liposomes and whether hHep1 interacts with cell membranes.

Material and methods

hHep1 production and purification

The His-tagged hHep1 recombinant protein was obtained from the expression vector pQE2::hHep1 and purified and quantified as described by Dores-Silva et al. (Dores-Silva et al. 2013). Recombinant HSPA9 was produced, purified and quantified as previously reported (Dores-Silva et al. 2015).

Production of liposomes and incorporation of hHep1

Liposomes were prepared as described by Lopez et al. (Lopez et al. 2016.). Briefly, 400 µg of cardiolipin (CL) or POPS (Avanti Polar Lipids) were dissolved in chloroform (10 mg mL^{-1}). After drying with nitrogen gas, the liposomes were resuspended in 120 µL of 50 mM Tris–HCl buffer (pH 7.5) and vortexed for 30 s every 5 min. This last process was repeated 6 times. Finally, the liposomes were extruded using a 100 nm membrane.

For incorporation assays, 400 µg of liposomes were incubated with hHep1 (20 µg) and/or HSPA9 (4 µg) in 50 mM Tris–HCl buffer (pH 7.5) for 30 min at 25 °C under agitation. This mixture was then centrifuged at 100,000 × g for 1 h at 4 °C. The pellet was resuspended in 300 µL of 100 mM Na_2CO_3 buffer (pH 11.5) and centrifuged at 100,000 × g for 1 h at 4 °C. Finally, the pellet was solubilized in 50 mM Tris–HCl buffer (pH 7.5). For electrophoretic separation the protein samples were solved in lithium dodecyl sulfate (LDS) sample buffer and part of them were resolved by commercial LDS-PAGE (ThermoFisher Scientific, Waltham, MA) and visualized by staining with Coomassie Brilliant Blue R-250 (ThermoFisher Scientific, Waltham, MA). As control, the protein load was also subjected to LDS-PAGE. The GelQuant program (http://biochemlabsolutions.com/GelQuantNET.html) was used to estimate the band intensity in the gel and the percentage of protein incorporated into the liposomes.

Structural study of hHep1 and its interaction with liposomes

The structural components involved in the interaction of hHep1 with liposomes were studied by circular dichroism (CD) and fluorescence emission spectroscopies. CD measurements were obtained using a J-815 spectropolarimeter (Jasco). Spectra of 10 µM hHep1 in 50 mM Tris–HCl buffer (pH 7.5) were obtained before and after 30 min of incubation at 25 °C with 1 mM POPS or CL. For all measurements, a circular quartz cuvette with an optical path of 0.01 cm was used, and 40 accumulations were performed. The resulting spectra were normalized to residual molar ellipticity ([θ]) according to the following equation:

$$[\theta] = \frac{\theta \times 100 \times MM}{n \times C \times l} \quad (1)$$

where θ is the sign of CD (degrees), MM is the protein molecular mass (kDa), n is the number of amino acid residues in the protein, l is the light path (cm), and C is the protein concentration (mg mL^{-1}).

Fluorescence emission measurements were taken on an F-4500 fluorimeter (Hitachi) using a quartz cuvette with an optical path of 1.0×0.2 cm after excitation at 295 nm. Spectra of hHep1 (10 µM) in 50 mM Tris–HCl buffer (pH 7.5) were obtained before and after 30 min of incubation at 25 °C with 1 mM POPS or CL. Data were collected between 310–420 nm and analyzed based on the maximum emission wavelength (λ_{max}) as well as spectral center of mass ($<\lambda>$), given by Eq. 2, between the spectra range of 310–390 nm.

$$<\lambda>=\frac{\Sigma\lambda i.Fi}{\Sigma Fi} \quad (2)$$

where λi is each wavelength where the fluorescence values (Fi) were measured.

Proteinase K digestion assays

Human Hep1 (70 µg) incorporated into liposomes (POPS or LC at 400 µg) was incubated with proteinase K (15 ng) for 1 h at 25 °C in 50 mM Tris–HCl buffer (pH 7.5). Then, the hHep1-liposome mixture was centrifuged at 100,000×g for 1 h at 4 °C and the pellets were ressuspended and resolved by LDS-PAGE as described above "Production of liposomes and incorporation of hHep1" section.

Thermodynamic study on the interaction of hHep1 with liposomes

A thermodynamic study on the interactions of hHep1 with liposomes was performed by isothermal titration calorimetry (ITC). The experiments were performed using an iTC200 microcalorimeter (GE Healthcare). Briefly, seventeen 2 µL aliquots of POPS or CL liposomes (3 mM lipids) were titrated into 203.8 µL of hHep1 (15 µM) at 25 °C. The curves were analysed to obtain the association constant (K_A), apparent enthalpy change (ΔH_{app}) and stoichiometry coefficient (*n*) using a non-linear regression equation implemented in the Microcal ITC200 Analysis Software 7.20 (an Origin-based program) offered by the supplier. The dissociation constant (K_D) was obtained as the inverse of K_A. The other thermodynamic parameters (ΔG_{app} and ΔS_{app}) were obtained by the relationship:

$$\Delta G_{app} = \Delta H_{app} - T\Delta S_{app} \quad (3)$$

where ΔG_{app} is the apparent Gibbs energy change, ΔH_{app} is the apparent enthalpy change, T is the temperature and ΔS_{app} is the apparent entropy change. Experiments were performed in triplicate.

Cytotoxicity assay

To verify the viability of cells treated with His-tagged hHep1, assays were performed using 3-(4,5-dimethylthiazol-2-yl)-2,5-diphenyl tetrazolium bromide (MTT). Human fibroblasts were cultivated in Dulbecco's modified Eagle's medium (DMEM) with 10% fetal bovine serum (FBS), L-glutamine (2 mM), penicillin (100 U/mL) and streptomycin (100 µg/mL). Cells were treated with hHep1 for 30 min and then incubated with MTT for 3 h at 37 °C. Then, the formazan crystals formed by viable cells were solubilized with dimethyl sulfoxide (DMSO). Absorbance measurements were performed at 570 nm using a plate reader (Thermo Scientific), and the cell viability percentage was evaluated compared to the viability of the control (untreated cells).

High-content imaging

The interaction of His-tagged hHep1 with the plasma membrane of human fibroblasts at different concentrations (2.5, 5 and 10 µM) was performed for 5, 10 and 30 min. After treatment, cells were incubated with mouse anti-Histag (Abclonal, AE003) and rabbit anti-hHep1 (Thermo Scientific, PA5-66527) primary antibodies and Alexa Fluor 488 goat anti-rabbit (Thermo Scientific, #2018207) or Alexa Fluor 488 goat anti-mouse (Abcam, ab6785) secondary antibodies. Images were obtained with an automated fluorescence microscope (ImageXpress Micro XLS Widefield High Content Analysis System, Molecular Devices). The fluorescence intensity of targeted hHep1 was quantified using MetaXpress software (Molecular Devices).

Confocal microscopy

To confirm that hHep1 was incorporated into cells (fibroblasts and U2OS cells), the cells were incubated with 5, 10 and 25 µM recombinant His-tagged purified protein for 30 min. After treatment, the cells were washed with PBS, fixed with 4% paraformaldehyde and blocked with 2% BSA. Recovery times (1 h and 2 h) in medium were also measured to verify the long-term interaction of hHep1 and the cell membrane. The influence of HSPA9 in the cellular incorporation of hHep1 was tested by incubating cells with their equimolar mixture at 5 µM for 30 min at 37 ºC in PBS. The cells were stained with anti-His (Abclonal, AE003l) or anti-hHep1 (Thermo Scientific, PA5-66527) primary antibodies and Alexa Fluor 488 goat anti-rabbit (Thermo Scientific, #2018207) or Alexa Fluor 594 donkey anti-rabbit (Abcam, ab150076) or Alexa Fluor 488 goat anti-mouse (Abcam, ab6785) secondary antibodies for visualization by confocal fluorescence microscopy. Cell nuclei were stained with DAPI. The analysis of the average fluorescence intensities of the slices of each image acquired along the z-axis was quantified, and the 3D projections and videos of the sequential images were reconstructed using ImageJ-Fiji software.

Western blotting

To confirm that recombinant His-tagged hHep1 was incorporated, Western blotting analysis was also performed.

U2OS cells were treated with 10 µM hHep1 for 30 min in PBS, and after 3 washes with PBS, they were submitted to recovery times of 30 min, 1 h and 2 h in Dulbecco's Modified Eagle Medium (DMEM). Cells were lysed in Laemmli buffer, and then the protein samples with b-mercaptoethanol were boiled for 5 min at 95 °C. After SDS−PAGE, proteins were transferred to a nitrocellulose membrane, blocked with milk and incubated with primary and secondary antibodies for Western blotting analysis. Quantification of the densitometry of the bands was performed using ImageJ software.

Statistics

All statistics were performed using Prism 5 software with one-way ANOVA, followed by Tukey's post hoc test. The experiments were carried out in three independent assays ($n=3$).

Results

hHep1 interacted with negatively charged liposomes

hHep1 was incubated with liposomes composed of POPS or CL as described in the Materials and Methods. After incubation, the liposomes were pelleted, and the incorporated protein was visualized by LDS-PAGE. As presented in Fig. 1a and b, hHep1 was associated with POPS and CL liposomes, respectively, suggesting that the protein interacted with both phospholipids, as previously shown (Dores-Silva et al. 2021b). The amount (percentage) of protein incorporated in each liposome was estimated based on the intensities of the bands of controls containing only hHep1 (Fig. 1c). Despite being a binary experiment, it can be concluded that hHep1 incorporation was similar for both CL and POPS liposomes.

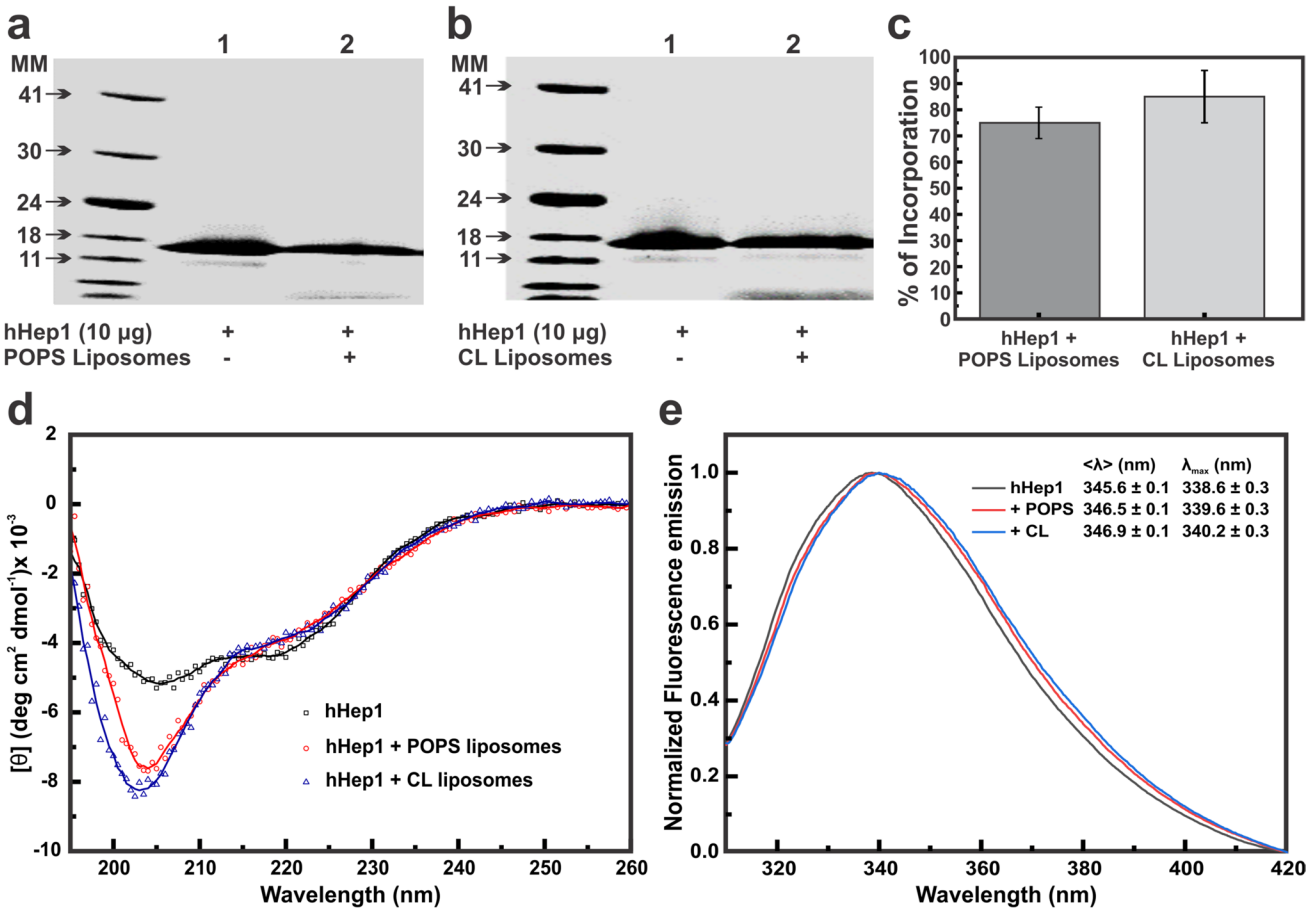

Fig. 1 hHep1 incorporation in negatively charged liposomes is efficient and causes conformational changes in its structure. After incubation, the LDS-PAGE gel reveals that hHep1 (10 µg) interacts with both POPS (**a**) and CL (**b**). Lanes 1 in the gel images are hHep1 load controls and lanes 2 are hHep1 pelleted that interacted with liposomes in the pulldown experiment. The amount of each band was evaluated by GelQuant program and their relative intensity is represented as the percentage of hHep1 incorporated in each liposome (**c**). Spectra of structural changes of the interaction of 10 µM hHep1 with POPS and CL evaluated by circular dichroism spectroscopy (**d**) and by tryptophan emission fluorescence (**e**). In the latter case, the respective calculated values of $<\lambda>$ are shown in the legend figure

This conclusion is in agreement with the similar affinity that hHep1 showed for both liposomes, as attested by ITC experiments (see below).

Interaction of hHep1 with liposomes modified its structure

We investigated whether the interaction with the negatively charged liposomes caused structural changes in hHep1 that were determined by CD and intrinsic emission fluorescence. Figure 1d indicates that hHep1 was folded according to that previously shown with a minimum around 205–207 nm and a shoulder at 220 nm which is according to the predicted model for it (Dores-Silva et al. 2013). The interaction of hHep1 with liposomes caused a large change in the CD spectrum, leading to an increase in its signal in the minimum range of 200–205 nm (Fig. 1d). In the presence of CL liposomes, hHep1 exhibited a slightly more negative CD signal at 200–205 nm than that of POPS liposomes. Since negative signals around 200 nm is related to random structure while 205–208 nm to organized structure (Correa et al. 2009; Seraphim et al. 2015), the CD spectra profile observed indicates that the organized structure was lost and a random structure was gained due to the liposome interactions. In contrast, no structural changes in the secondary structure level were observed for the interaction of HSP70 with negatively charged liposomes (Dores-Silva et al. 2020a, b, 2021b).

The changes at the secondary structure level were supported by the fluorescence emission spectra of 10 µM hHep1 in the presence of the POPS or CL liposomes (Fig. 1e), which reported small changes in the local tertiary structure level. In the absence of liposomes, hHep1 fluorescence emission spectra exhibited features of a folded protein in which a single tryptophan is partially exposed to the solvent with a λ_{max} of 338.6 ± 0.3 nm and a $<\lambda>$ value of 345.6 ± 0.1 nm (Dores-Silva et al. 2013). The normalized spectra (Fig. 1e) in the presence of the liposomes showed a slight, but technically significant, redshift in the intrinsic fluorescence emission spectra of hHep1. In the presence of CL liposomes, λ_{max} and $<\lambda>$ were 340.2 ± 0.3 nm and 346.9 ± 0.1 nm, respectively. The λ_{max} and $<\lambda>$ values registered in the presence of POPS liposomes were 339.6 ± 0.3 nm and 346.5 ± 0.1 nm, respectively. Based on these values, we conclude that CL liposomes caused more changes in the hHep1 structure than POPS liposomes. The presence of the liposomes did not lead to complete hHep1 unfolding since both λ_{max} and $<\lambda>$ registered are in agreement with tryptophan partially exposed to the solvent (Dores-Silva et al. 2013; Batista et al. 2015). In contrast to that observed for human HSP70 (Dores-Silva et al. 2020a, b, 2021b), the secondary and local tertiary structure evaluations indicated that the interactions with POPS and CL caused significant changes in the hHep1 structure with a reduction in its structural content but did not cause hHep1 to completely unfold.

On the same line, Fig. 2 suggests that interaction with liposomes did not largely protect hHep1 from proteolysis by proteinase K. The results indicated that the interaction between hHep1 and liposomes occurs mostly peripherally, and the protein is not greatly inserted into the lipid bilayer. This mechanism is different from that observed for HSPA9 and other HSP70s, since under similar conditions, these chaperones were well inserted into liposomes (Dores-Silva et al. 2020b). However, comparing the intensities of the

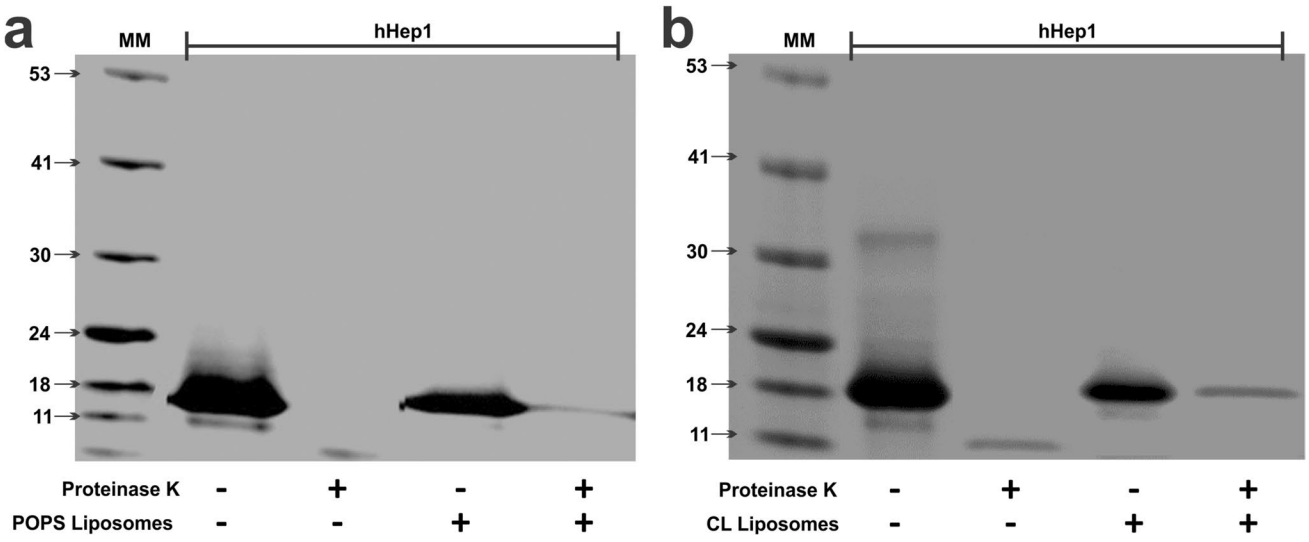

Fig. 2 hHep1 interaction with lipid bilayer is peripherally. LDS-PAGE gels showing the interaction of hHep1 with POPS (**a**) and CL (**b**) in the presence and absence of proteinase K

hHep1 bands after association with POPS and CL liposomes in the absence or presence of proteinase K after 1 h of incubation, we can conclude that a small part of hHep1 was resistant to proteinase K activity. A more intense band was observed under the condition in which hHep1 interacts with CL liposomes in the presence of proteinase (Fig. 2b), suggesting that hHep1 was more resistant to proteinase K when prepared in the CL bilayer than in the POPS bilayer.

Interactions between liposomes and hHep1 were enthalpically and entropically driven

The thermodynamic factors that affect the interaction between hHep1 and liposomes were investigated by ITC. Figure 3 presents representative isothermograms obtained from the liposome titrations into the hHep1 solutions, and Table 1 summarizes all the thermodynamic parameters obtained from the nonlinear fitting using the simplest model for interaction. The isothermogram profiles indicated that the interactions of POPS and CL with hHep1 were exothermic processes. However, compared to POPS liposomes, the interaction of hHep1 with CL liposomes led to 2.5-fold greater heat release, probably because charge-related interactions formed more efficiently. Despite the exothermic profiles, both interactions yielded similar ΔG_{app} values, indicating that the affinities and association/dissociation

Table 1 Thermodynamic parameters for the interaction of POPS or CL liposomes with hHep1 amounted by ITC at 25 ºC. Data from the average of three different titrations

Interactors	POPS liposomes → hHep1	CL liposomes → hHep1
ΔG_{app} (cal/mol)	-6500 ± 100	-6720 ± 60
ΔH_{app} (cal/mol)	-730 ± 50	-1870 ± 50
ΔS_{app} (cal/mol/K)	+ 19.5 ± 0.6	+ 16.3 ± 0.2
$-T\Delta S_{app}$ (cal/mol)	-5800 ± 200	-4850 ± 60
K_{Aapp} (M^{-1})	$(6 \pm 1) \times 10^{+4}$	$(8.4 \pm 0.9) \times 10^{+4}$
K_{Dapp} (μM)	17 ± 3	12 ± 1
n (lipids per hHep1)	24 ± 1	19.8 ± 0.5

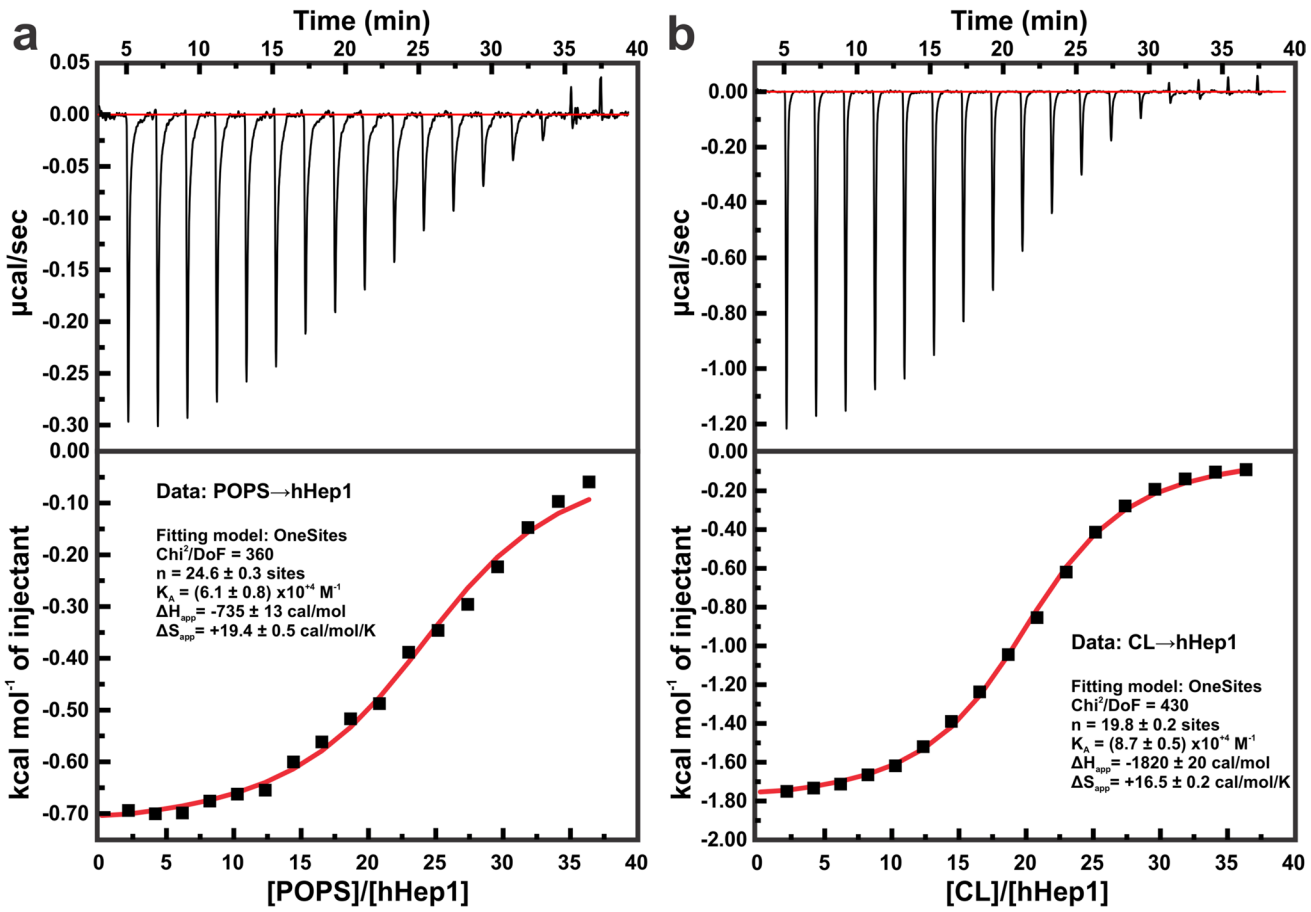

Fig. 3 Calorimetric study of the interaction of liposomes with hHep1. Representatives isothermograms of the interaction between hHep1 and POPS (**a**) and hHep1 and CL (**b**). The thermodynamic parameters (ΔH_{app}, K_A and *n*) were obtained by a non-linear fitting equation using the One Bind site model in the Origin 7.0 based analysis program

constants were similar (Table 1). In addition, the positive value obtained for ΔS_{app} indicated that the interactions were also driven by entropy changes, probably due to dehydration and other events that led to a state of greater degree of freedom. Therefore, hHep1 interactions with both negatively charged liposomes were driven by changes in enthalpy and entropy. The stoichiometry coefficients obtained (Table 1) also suggest that the liposomes contain a similar number of lipids to interact with hHep1.

Interestingly, compared to HSPA9, hHep1 has been shown to exhibit higher affinity for negatively charged liposomes (Dores-Silva et al. 2020b). The interactions of hHep1 and HSPA9 with POPS liposomes were enthalpically and entropically driven. Nevertheless, HSPA9 and hHep1 interaction with CL liposomes presented divergent thermodynamic signatures, since CL interaction with HSPA9 had an opposite ΔH_{app} (Dores-Silva et al. 2020b).

hHep1 was incorporated into the plasma membrane of human fibroblasts

Previous results from our group showed that hHep1 interacts with various types of liposomes composed of different lipids (Dores-Silva et al. 2021b), suggesting that hHep1 may also interact with cell membranes. To verify this interaction, assays were performed with human fibroblasts treated with purified recombinant His-tagged hHep1. First, it was demonstrated that hHep1 in the concentration range between 5–80 μM presented a survival percentage similar to the untreated cell (Fig. 4a), indicating that there was no cell death with these concentrations used and 30 min of incubation.

Confocal microscopy assays were also performed to further confirm whether hHep1 interacts with the plasma membrane and/or incorporates into the cells. As a result, His-tagged hHep1 interacted with the fibroblast membrane and was further translocated into the cytosol. Figure 4b shows representative images of hHep1 stained in green and the nuclei in blue. Figure 4c represents statistics for the quantification of each image stack, showing a significant increase in hHep1 at 10 and 25 μM compared to untreated cells. The z-stacks images were performed in order to evaluate the hHep1 presence inside cells. Along the z-axis, it can be observed that the average fluorescence intensity (IFm) in the cells increased as they approached the nucleus, with a subsequent decrease in this intensity (Fig. 4d). The stacks obtained and quantified from each image were also reconstructed in 3D projection videos and images to demonstrate hHep1 incorporation along the z-axis by fibroblasts (Figure S1 and videos V1-V3, Supplementary information).

Western blotting analysis was performed to confirm hHep1 incorporation by U2OS cells after 30 min of treatment, and hHep1 remained there for at least 120 min after incubation (Fig. 4f and g). In addition, 3D stacking images (Fig. 4e and S2, Supplementary information) were performed to further demonstrate hHep1 incorporation into U2OS cells. The interaction of hHep1 with cell membrane was also confirmed by live confocal imaging of fibroblasts after treatments with FITC-labeled hHep1 during 10 and 20 min. FITC-labeled hHep1 had similar membrane interaction in both incubation periods as showed in Figure S2 and videos V4 and V5 (Supplementary information).

A previous assay was performed to verify the concentration and incubation period of hHep1 that interacted with cells. Figure S3 indicates that His-tagged hHep1 was incorporated into cells, as observed by the increase in fluorescence of stained protein with anti-hHep1 along the concentrations and incubation periods used. It was also performed using anti-His staining, and the results corroborated anti-hHep1 labelling (Figure S4, Supplementary information). As a control, the recombinant protein His-tagged luciferase fused to myc (LUC-Myc) was used to show that it did not interact with the fibroblast membranes and was not incorporated by the cells (Figure S5, Supplementary information). This result demonstrates that hHep1 specifically interacts with fibroblasts (Fig. 4a-c) and with U2OS cell membranes (Fig. 4d).

Combining hHep1/HSPA9 enhanced hHep1 interaction with lipids bilayer

In a previous study, we found that hHep1 and HSPA9 interacted mainly with negatively charged liposomes and liposomes mimicking the inner mitochondrial membrane (Dores-Silva et al. 2020b, 2021b). On the other hand, hHep1 exhibited only a slight preference for negatively charged liposomes (Dores-Silva et al. 2021b). Based on these data, we investigated whether the incorporation of both proteins in a liposome that mimics the inner mitochondrial membrane is influenced by each protein. For that, we prepared a liposome from a mixture of POPS, CL, POPC and POPE lipids in proportion that mimicked the chemical environment of the inner mitochondrial membrane. HSPA9 (~ 56 nM) was combined with hHep1 (~ 1.3 μM) in a 1:25 molar ratio, and the mixture was incubated with the lipid bilayer, where they probably formed a complex because their K_D lies in the submicromolar range (Dores-Silva et al. 2021b). After that, the proteins were pulled down with the liposomes and resolved by LDS-PAGE (Fig. 5a). Figure 5b indicated that a proportional amount of each of them was incorporated in the liposome.

Due to the lipid composition, both proteins interacted with the liposome mixture (Dores-Silva et al. 2020b, 2021b) with uptake rates for HSPA9 and hHep1 alone at approximately 60%. When we considered their mixture to form a complex, it was observed that the protein

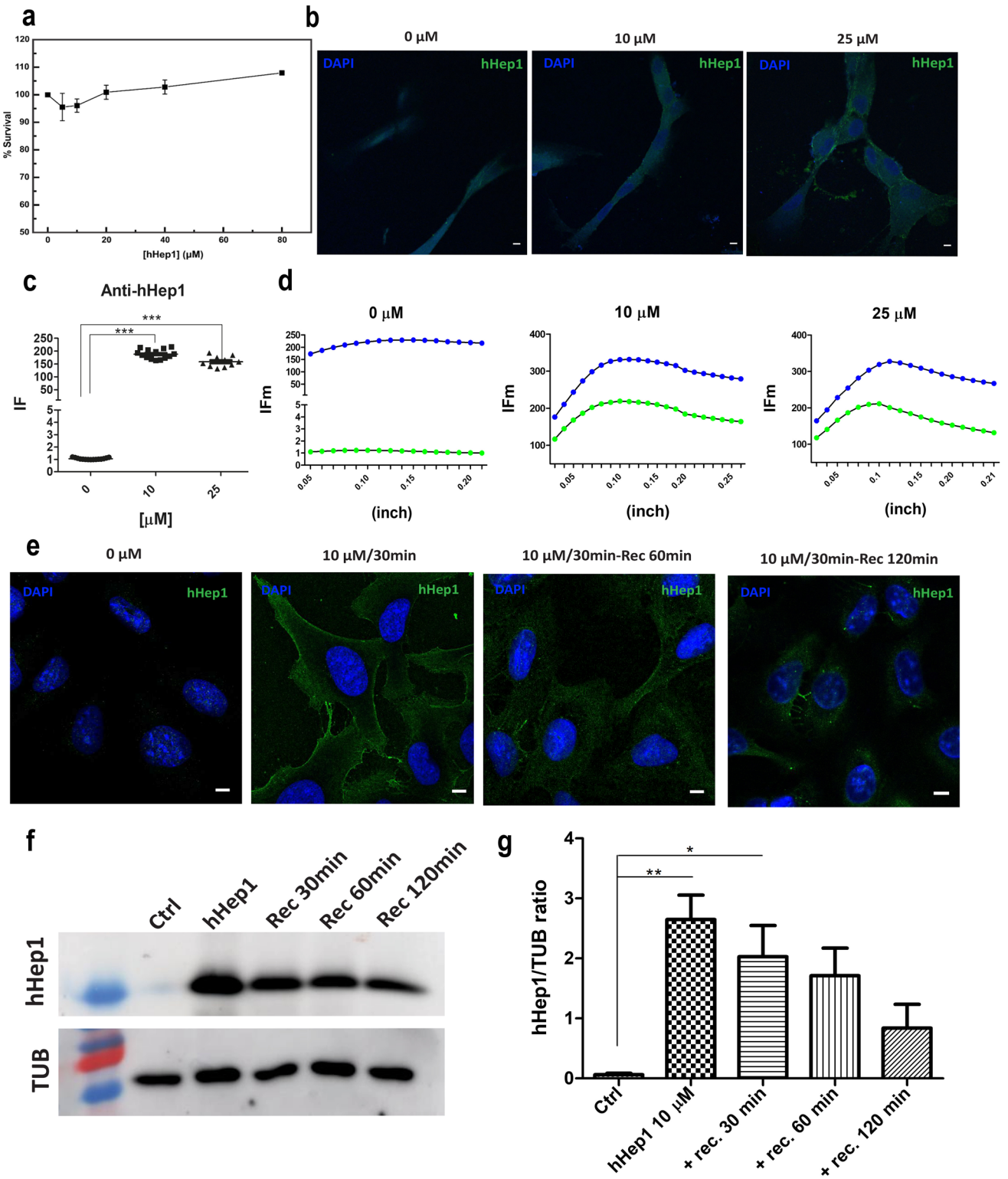

incorporation rates increased by approximately 20% (Fig. 5a-b). We confirmed that hHep1 cell uptake was favored by incubating the recombinant HSPA9 with hHep1. Confocal images quantification showed that around 50% more of hHep1 was incorporated in cells treated with hHep1/HSPA9 compared to the treatment with recombinant hHep1 only (Fig. 5c-d). Therefore, we can infer that the interaction between HSPA9 and hHep1 is beneficial for inserting hHep1 into the lipid bilayer.

◂**Fig. 4** hHep1 interacts with cell plasma membrane, incorporating in human fibroblasts and in U2OS cells (**a**) Viability of human fibroblasts treated with purified recombinant hHep1 His-tag protein analyzed by MTT assay performed in duplicate. The absorbance measurements at 570 nm were converted into percentage for survival rate compared to control (100% survival). (**b**) Representative confocal images of human fibroblasts stained with anti-hHep1 antibody (green) and nuclei stained with DAPI (blue). Cells were treated with different hHep1 concentrations (0, 10 and 25 μM) for 30 min. (**c**) Graph represents the quantification of green fluorescence intensities (anti-hHep1) in each slice field compared to control using ANOVA followed by Tukey's test (***$p < 0.001$). **(d)** Graphs of the mean fluorescence intensities (IFm) in the green channel (FITC) of the hHep1 along the image slices (z-inch axis) obtained under a confocal microscope. DAPI signal is represented in blue. **(e)** Representative confocal images of U2OS cells stained with anti-hHep1 antibody (green) and nuclei stained with DAPI (blue). Cells were treated with hHep1 at 10 μM of concentration for 30 min (10 μM/30 min) in PBS and recovery time at 1 h (10 μM/30 min-Rec 1 h) and 2 h (10 μM/30 min-Rec 2 h) in medium. **(f)** Western blotting of U2OS cells: non treated (Ctrl), hHep1 at 10 μM of concentration for 30 min in PBS (hHep1) and recovery time at 30 min (Rec 30 min), 60 min (Rec 60 min) and 120 min (Rec 120 min) in medium. **(g)** Graphs of the densitometry ratio (hHep1/TUB) in three independent assays ($n = 3$). The results of quantification were compared using ANOVA followed by Tukey's test (*$p < 0.05$ and **$p < 0.01$)

Discussion

Membrane proteins are surrounded by lipids by a nonspecific association, although some protein regions may display higher affinity with anionic lipids (Lee 2005). HSP70s have been proposed to modulate membrane properties and functions, such as fluidity and permeability (Horváth et al. 2008). The interaction between HSP70s and membranes may depend on the nature of the biological membranes and the protein content. Several studies have shown that human HSP70s can be incorporated into negatively charged liposomes with medium to high affinity (Arispe et al. 2004; Armijo et al. 2014; Dores-Silva et al. 2020a, b, 2021a). The monomeric state of HSPA9 is essential for its role in subcellular compartments, indicating that the interaction of HSP70 with lipids corroborates its protein functions.

Previous results from our group showed that hHep1 interacted with HSP70s, impairing the formation of HSPA9 and HSPA1A supramolecular assemblies (SMAs) under thermal conditions and stimulating the ATPase activity of these proteins. In addition, hHep1 remodels HSPA9 and HSPA1A SMAs into smaller states (Dores-Silva et al. 2021b). As the interaction of hHep1 with HSPA9 is critical for its stability and function (Burri et al. 2004; Dores-Silva et al. 2015; Dores-Silva et al. 2021a; Dores-Silva et al. 2013; Sichting et al. 2005; Szklarz et al. 2005), our data raise a question regarding whether hHep1 is present on the cell surface in complex with HSPA9, where it could assist its functions (Dores-Silva et al. 2020b; Kiraly et al. 2020). In this context, this study aimed to further elucidate how hHep1 interacts with liposomes and plasma membranes.

We report that hHep1 interacts with liposomes and remains partially structured. Notably, its CD spectrum and its spectral center of mass incurred punctual changes. Electrophoresis gels were performed to verify the percentage of incorporation and clearly indicate that hHep1 can interact with POPS and CL liposomes, demonstrating that hHep1 exhibits similar affinities for both liposomes formed by POPS and CL, which was confirmed by ITC experiments. In addition, the interactions of hHep1 with these liposomes were enthalpically and entropically directed. The most conserved region among hHep1 and yHep1 is the core region containing the zinc finger domain, where the four cysteines responsible for coordinating the zinc ion are located. Our results suggested that the interaction between hHep1 and liposomes must occur via this core region, and the protein is not greatly inserted into the lipid bilayer because of its conservation and susceptibility to proteinase K, respectively.

We also demonstrated that hHep1 enhanced HSPA9 incorporation into liposomes, suggesting that both proteins cooperate and achieve better lipid bilayer interactions or binding affinity of the complex than that achieved by each protein separately (Fig. 4). It has been shown that the complexity of the plasma membrane favored the passage of cyclic peptides, while they only interacted peripherally with artificial liposomes (Ovadia et al. 2011). Something similar may occur with hHep1; in other words, the plasma membrane environment and components are probably needed for the incorporation and accumulation of hHep1 inside cells. Earlier studies demonstrated that HSP70s directly interact with lipid bilayers and indicated that HSP70s may play a role in the translocation of other proteins across membranes (Arispe et al. 2002). In this context, our results showed that hHep1 can be involved in this translocation role together with HSPA9.

The plasma membrane is composed of more than lipids. It was estimated that the ratio in the number of proteins per lipid is 1:40, suggesting that a large amount of proteins are embedded in the membrane (Engelman 2005). One of those proteins is the HSP70 family, which is found in close proximity or in association with cellular membranes (Arispe et al. 2002; De Maio and Hightower 2021a). In addition, HSP70s were found in the plasma membrane of tumour cells (Camins et al. 1995; Kaur et al. 1998). In particular, HSP70 isoforms are found in almost all subcellular compartments and are also associated with plasma membrane microdomains called “lipid rafts” (Broquet et al. 2003). Mazkereth and coworkers also showed that HSPA9 translocates to the cell surface upon complement-induced stress, suggesting that the mechanisms by which HSPA9 incorporates in the

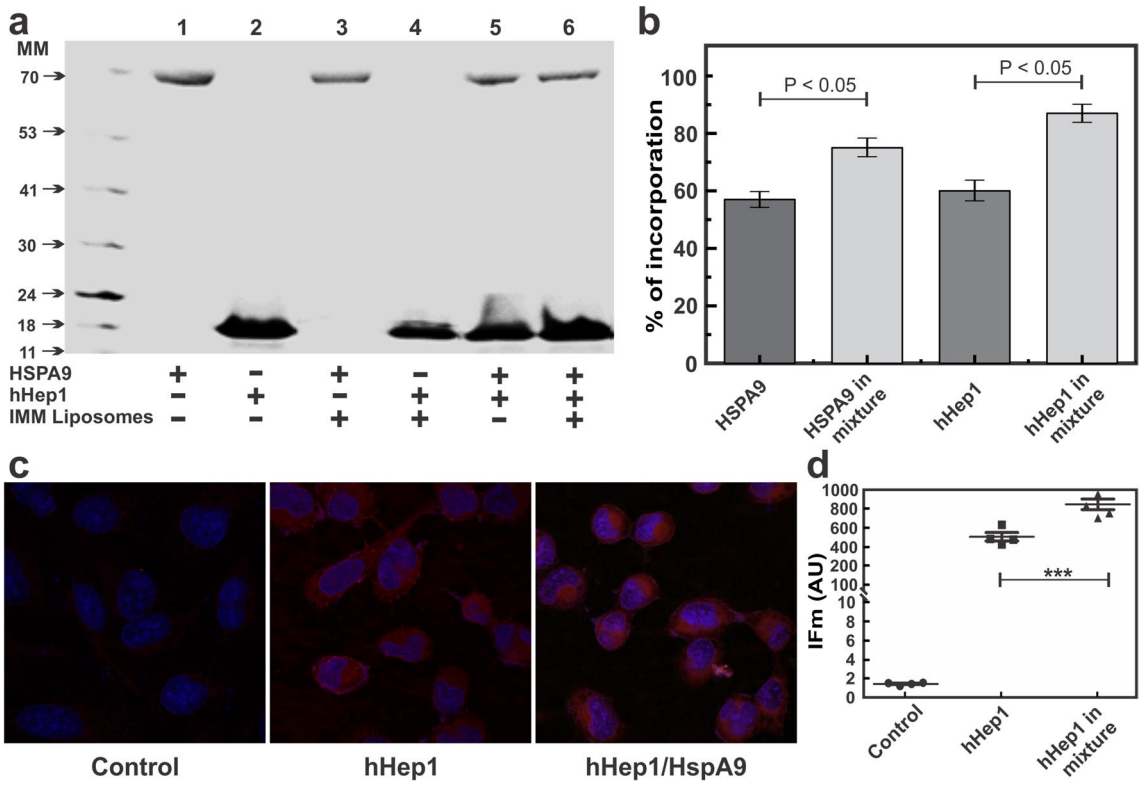

Fig. 5 Formation of the hHep1/HSPA9 complex and interaction with lipid bilayer and cell membrane. **(a)** Study of the interaction of hHep1 with HSPA9 in the presence and absence of a mixture of liposomes that mimic the inner mitochondrial membrane (POPS 3%, CL 18%, POPC 45% and POPE 34%). Representative image of LDS-PAGE. 1: HSPA9 (loading control at ~ 56 nM). 2: hHep1 (loading control at ~ 1.3 µM). 3 HSPA9 pulled down with the mixture of liposomes (POPS 3%, CL 18%, POPC 45% and POPE 34%). 4: hHep1 pulled down with the mixture of liposomes. 5: HSPA9 and hHep1 pulled down. 6: HSPA9 and hHep1 pulled down with the mixture of liposomes. (**b**) The GelQuant software was used to analyze the intensity of the bands in the gel and, consequently, estimate the percentage of hHep1 and HSPA9 incorporated in each condition. Experiment performed in triplicate. (**c**) Representative confocal images of U2OS cells stained with anti-hHep1 antibody (red) and nuclei stained with DAPI (blue). Cells were treated with hHep1 at 5 µM of concentration for 30 min, or with both hHep1/HSPA9 at 1:1 molar ratio for 30 min in PBS. (**d**) Graph represents the quantification of red fluorescence intensities (anti-hHep1) increment of each slice field in hHep1 treatment compared to hHep1/HSPA9 treatment using ANOVA followed by Tukey's test (***$p < 0.001$)

plasma membrane involve lipid rafts (Mazkereth et al. 2016). Lipid rafts are sphingolipids and cholesterol-rich regions in the plasma membrane that concentrate diverse proteins with important roles in cellular processes (Simons & Ikonen 1997). Here, we suggest that hHep1 may be incorporated by cells after interacting with HSP70s present in the plasma membrane. Apart from this hypothesis, our published *in vitro* results indicate that hHep1 is capable of interacting with liposomes prepared with different types of lipids (Dores-Silva et al 2021a, b). Based on our results we mainly believe that hHep1 is capable of interacting directly with lipids in the plasma membrane. Finally, the results obtained contribute to elucidating the interaction mechanisms of hHep1 with lipid bilayers and demonstrated the potential of incorporating hHep1 through cell membranes.

Supplementary Information The online version contains supplementary material available at https://doi.org/10.1007/s12192-023-01394-1.

Acknowledgements This work was supported by Fundação de Amparo à Pesquisa do Estado de São Paulo (FAPESP) grants (#2012/50161-8, #2014/16646-0, #2016/22477-1, #2017/07335-9, #2017/26131-5, #2019/22422-0 and #2021/12775-3), by the Conselho Nacional de Pesquisa e Desenvolvimento (CNPq) grant (grant #303262/2018-4 and #310927/2021-8), by the National Institutes of Health (NIH) grants: R01 GM098455-04 and R01 GM114473-01, by MUR (Departments of excellence 2018-2022; E91I18001480001) and the University of Modena and Reggio Emilia (Unimore FAR2020 Mission Oriented).

Data Availability Data will be made available on request.

Declarations

Conflict of interest The authors declare no conflict of interest.

References

Araujo TLS, Venturini G, Moretti AIS, Tanaka LY, Pereira AC, Laurindo FRM (2019) Cell-surface HSP70 associates with

thrombomodulin in endothelial cells. Cell Stress Chaperones 24:273–282. https://doi.org/10.1007/s12192-018-00964-y

Arispe N, Doh M, De Maio A (2002) Lipid interaction differentiates the constitutive and stress-induced heat shock proteins Hsc70 and Hsp70. Cell Stress Chaperones 7(4):330. https://doi.org/10.1379/1466-1268(2002)007%3c0330:lidtca%3e2.0.co;2

Arispe N, Doh M, Simakova O, Kurganov B, De Maio A (2004) Hsc70 and Hsp70 interact with phosphatidylserine on the surface of PC12 cells resulting in a decrease of viability. FASEB 18:1636–1645. https://doi.org/10.1096/fj.04-2088com

Armijo G, Okerblom J, Cauvi DM, Lopez V, Schlamadinger DE, Kim J, Arispe N, De Maio A (2014) Interaction of heat shock protein 70 with membranes depends on the lipid environment. Cell Stress Chaperones 19:877–886. https://doi.org/10.1007/s12192-014-0511-x

Bailone RL, Fukushima S, Aguiar D, Borra LK (2022) Mortalin as a biomarker disease and therapeutic target. Sci J Biol 5(1):1–09. https://doi.org/10.37871/sjb.id25

Baseler WA, Croston TL, Hollander JM (2012) Functional characteristics of mortalin. Mortalin Biol: Life, Stress and Death 9789400730274:55–80. https://doi.org/10.1007/978-94-007-3027-4

Batista FA, Gava LM, Pinheiro GM, Ramos CH, Borges JC (2015) From conformation to interaction: techniques to explore the Hsp70/Hsp90 network. Curr Protein Pept Sci 16:735–753

Broquet AH, Thomas G, Masliah J, Trugnan G, Bachelet M (2003) Expression of the molecular chaperone Hsp70 in detergent-resistant microdomains correlates with its membrane delivery and release. J Biol Chem 278(24):21601–21606. https://doi.org/10.1074/JBC.M302326200

Burri L, Vascotto K, Fredersdorf S, Tiedt R, Hall MN, Lithgow T (2004) Zim17, a novel zinc finger protein essential for protein import into mitochondria. J Biol Chem 279:50243–50249

Camins A, Diez-Fernandez C, Camarasa J, Escubedo E (1995) Cell surface expression of heat shock proteins in dog neutrophils induced by mitochondrial benzodiazepine receptor ligands. Immunopharmacology 29(2):159–166. https://doi.org/10.1016/0162-3109(94)00055-K

Chouchane L, Bowers FS, Sawasdikosol S, Simpson RM, Kindt TJ (1994) Heat-shock proteins expressed on the surface of human T Cell leukemia virus Type I-infected cell lines induce autoantibodies in rabbits. J Infect Dis 169(2):253–259. https://doi.org/10.1093/INFDIS/169.2.253

Correa D, Henrique C, Ramos I, Correa DHA, Ramos CHI (2009) The use of circular dichroism spectroscopy to study protein folding, form and function. African J Biochem Res 3(5):164–173

De Maio A (1999) Heat shock proteins: facts, thoughts, and dreams. Shock 11:1–12

De Maio A, Hightower LE (2021a) The interaction of heat shock proteins with cellular membranes: an historical perspective. Cell Stress Chaperones 26:769–783. https://doi.org/10.1007/s12192-021-01228-y

De Maio A, Hightower LE (2021b) Heat shock proteins and the biogenesis of cellular membranes. Cell Stress Chaperones 26:15–18. https://doi.org/10.1007/s12192-020-01173-2

Dores-Silva PR, Minari K, Ramos CHI, Barbosa LRS, Borges JC (2013) Structural and stability studies of the human mtHsp70-escort protein 1: an essential mortalin co-chaperone. Int J Biol Macromol 1(56):140–148. https://doi.org/10.1016/j.ijbiomac.2013.02.009

Dores-Silva PR, Barbosa LR, Ramos CH, Borges JC (2015) Human mitochondrial Hsp70 (mortalin): shedding light on ATPase activity, interaction with adenosine nucleotides, solution structure and domain organization. PLoS One 10:e0117170

Dores-Silva PR, Cauvi DM, Coto ALS, Kiraly VTR, Borges JC, De Maio A (2020a) Interaction of HSPA5 (Grp78, BIP) with negatively charged phospholipid membranes via oligomerization involving the N-terminal end domain. Cell Stress Chaperones 25:979–991

Dores-Silva PR, Cauvi DM, Kiraly VTR, Borges JC, De Maio A (2020b) Human HSPA9 (mtHsp70, mortalin) interacts with lipid bilayers containing cardiolipin, a major component of the inner mitochondrial membrane. Biochim Biophys Acta Biomembr 1862:183436

Dores-Silva PR, Cauvi DM, Coto ALS, Silva NSM, Borges JC, De Maio A (2021a) Human heat shock cognate protein (HSC70/HSPA8) interacts with negatively charged phospholipids by a different mechanism than other HSP70s and brings HSP90 into membranes. Cell Stress Chaperones 26:671–684

Dores-Silva PR, Kiraly VTR, Moritz MNO, Serrao VHB, Dos Passos PMS, Spagnol V, Teixeira FR, Gava LM, Cauvi DM, Ramos CHI et al (2021b) New insights on human Hsp70-escort protein 1: chaperone activity, interaction with liposomes, cellular localizations and HSPA's self-assemblies remodeling. Int J Biol Macromol 182:772–784

Engelman DM (2005) Membranes are more mosaic than fluid. Nature 438:578–580. https://doi.org/10.1038/nature04394

Ferrarini M, Heltai S, Zocchi MR, Rugarli C (1992) Unusual expression and localization of heat-shock proteins in human tumor cells. Int J Cancer 51(4):613–619. https://doi.org/10.1002/IJC.2910510418

Goding JW (1976) Conjugation of antibodies with fluorochromes: modifications to the standard methods. J Immunol Methods 13(3–4):215–226. https://doi.org/10.1016/0022-1759(76)90068-5

Hartl FU (1996) Molecular chaperones in cellular protein folding. Nature 381:571–580

Hartl FU, Hayer-Hartl M (2002) Molecular chaperones in the cytosol: from nascent chain to folded protein. Science 295:1852–1858. https://doi.org/10.1126/science.1068408

Heufelder AE, Wenzel BE, Bahn RS (1992) Cell surface localization of a 72 kilodalton heat shock protein in retroocular fibroblasts from patients with Graves' ophthalmopathy. J Clin Endocrinol Metab 74(4):732–736. https://doi.org/10.1210/JCEM.74.4.1548335

Horváth I, Multhoff G, Sonnleitner A, Vígh L (2008) Membrane-associated stress proteins: more than simply chaperones. Biochimica et Biophysica Acta (BBA) - Biomembranes 1778(7–8):1653–1664. https://doi.org/10.1016/J.BBAMEM.2008.02.012

Kampinga HH, Craig EA (2010) The HSP70 chaperone machinery: J proteins as drivers of functional specificity. Nat Rev Mol Cell Biol 11(579):592

Kaul SC, Deocaris CC, Wadhwa R (2007) Three faces of mortalin: a housekeeper, guardian and killer. Exp Gerontol 42(4):263–274. https://doi.org/10.1016/J.EXGER.2006.10.020

Kaur J, Das SN, Srivastava A, Ralhan R (1998) Cell surface expression of 70 kDa heat shock protein in human oral dysplasia and squamous cell carcinoma: correlation with clinicopathological features. Oral Oncol 34(2):93–98. https://doi.org/10.1016/S1368-8375(97)00055-9

Kiraly VTR, Dores-Silva PR, Serrão VHB, Cauvi DM, De Maio A, Borges JC (2020) Thermal aggregates of human mortalin and Hsp70-1A behave as supramolecular assemblies. Int J Biol Macromol 146:320–331. https://doi.org/10.1016/j.ijbiomac.2019.12.236

Lee AG (2005) How lipids and proteins interact in a membrane: a molecular approach. Mol BioSyst 1:203–212. https://doi.org/10.1039/b504527d

Lingwood D, Simons K (2010) Lipid rafts as a membrane-organizing principle. Science 327(5961):46–50. https://doi.org/10.1126/Science

Lopez V, Cauvi DM, Arispe N, De Maio A (2016) Bacterial Hsp70 (DnaK) and mammalian Hsp70 interact differently with lipid

membranes. Cell Stress Chaperones 21:609–616. https://doi.org/10.1007/s12192-016-0685-5
Lynn KS, Peterson RJ, Koval M (2020) Ruffles and spikes: control of tight junction morphology and permeability by claudins. Biochim Biophys Acta Biomembr 1862:183339
Mazkereth N, Rocca F, Schubert JR, Geisler C, Hillman Y, Egner A, Fishelson Z (2016) Complement triggers relocation of Mortalin/GRP75 from mitochondria to the plasma membrane. Immunobiology 221(12):1395–1406. https://doi.org/10.1016/J.IMBIO.2016.07.005
Multhoff G, Botzler C, Wiesnet M, Müller E, Meier T, Wilmanns W, Issels RD (1995) A stress-inducible 72-kDa heat-shock protein (HSP72) is expressed on the surface of human tumor cells, but not on normal cells. Intl J Cancer 61:272–279. https://doi.org/10.1002/ijc.2910610222
Ovadia O, Greenberg S, Chatterjee J, Laufer B, Opperer F, Kessler H, Gilon C, Hoffman A (2011) The effect of multiple N-methylation on intestinal permeability of cyclic hexapeptides. Mol Pharmaceutics 8:479–487. https://doi.org/10.1021/mp1003306
Ran Q, Wadhwa R, Kawai R, Kaul SC, Sifers RN, Bick RJ, Smith JR, Pereira-Smith OM (2000) Extramitochondrial localization of mortalin/mthsp70/PBP74/GRP75. Biochem Biophys Res Commun 275(1):174–179. https://doi.org/10.1006/BBRC.2000.3237
Salibe-Filho W, Araujo TLS, Melo EG, Coimbra LBCT, Lapa MS, Acencio MMP, Freitas-Filho O, Capelozzi VL, Teixeira LR, Fernandes CJCS, Jatene FB, Laurindo FRM, Terra-Filho M (2020) Shear stress-exposed pulmonary artery endothelial cells fail to upregulate HSP70 in chronic thromboembolic pulmonary hypertension. PLoS One. https://doi.org/10.1371/journal.pone.0242960
Samborski P, Grzymisławski M (2015) The role of HSP70 heat shock proteins in the pathogenesis and treatment of inflammatory bowel diseases. Adv Clin Exp Med 24(3):525–530. https://doi.org/10.17219/ACEM/44144
Schilling D, Gehrmann M, Steinem C, De Maio A, Pockley AG, Abend M, Molls M, Multhoff G (2009) Binding of heat shock protein 70 to extracellular phosphatidylserine promotes killing of normoxic and hypoxic tumor cells. FASEB J 23:2467–2477. https://doi.org/10.1096/fj.08-125229
Seraphim TV, Gava LM, Mokry DZ, Cagliari TC, Barbosa LRS, Ramos CHI et al (2015) The C-terminal region of the human p23 chaperone modulates its structure and function. Arch Biochem Biophys 565:57–67. https://doi.org/10.1016/j.abb.2014.10.015
Sichting M, Mokranjac D, Azem A, Neupert W, Hell K (2005) Maintenance of structure and function of mitochondrial Hsp70 chaperones requires the chaperone Hep1. EMBO J 24:1046–1056
Simons K, Ikonen E (1997) Functional rafts in cell membranes. Nature Macmillan Publishers Ltd, 387
Smulders L, Daniels AJ, Plescia CB, Berger D, Stahelin RV, Nikolaidis N (2020) Characterization of the relationship between the chaperone and lipid-binding functions of the 70-kDa heat-shock protein, HspA1A. Mdpi.Com. https://doi.org/10.3390/ijms21175995
Szklarz LKS, Guiard B, Rissler M, Wiedemann N, Kozjak V, van der Laan M, Lohaus C, Marcus K, Meyer HE, Chacinska A et al (2005) Inactivation of the mitochondrial heat shock protein Zim17 leads to aggregation of matrix Hsp70s followed by pleiotropic effects on morphology and protein biogenesis. J Mol Biol 351:206–218
The, T. H, Feltkamp TEW (1970) Conjugation of fluorescein isothiocyanate to antibodies I. Experiments on the conditions of conjugation. Immunology 18:865
Turturici G, Sconzo G, Geraci F (2011) Hsp70 and its molecular role in nervous system diseases. Biochem Res Int 2011. https://doi.org/10.1155/2011/618127
Vega VL, Rodríguez-Silva M, Frey T, Gehrmann M, Diaz JC, Steinem C, Multhoff G, Arispe N, De Maio A (2008) Hsp70 translocates into the plasma membrane after stress and is released into the extracellular environment in a membrane-associated form that activates macrophages. J Immunol 180:4299–4307. https://doi.org/10.4049/jimmunol.180.6.4299
Wadhwa R, Taira K, Kaul SC (2002) An Hsp70 family chaperone, mortalin/mthsp70/PBP74/Grp75: what, when, and where? Cell Stress Chaperones 7(3):309. https://doi.org/10.1379/1466-1268
Yun C-O, Bhargava P, Na Y, Lee J-S, Ryu J, Kaul SC, Wadhwa R (2017) Relevance of mortalin to cancer cell stemness and cancer therapy. https://doi.org/10.1038/srep42016